Available online at www.sciencedirect.com
SCIENCE DIRECT®
Chemical Physics 311 (2005) 307–319
Chemical Physics
www.elsevier.com/locate/chemphys

Fine-structure vibronic spectra and NH-phototautomerism in free-base unsubstituted 2,3-naphthalocyanine in naphthalene at 6 K

S.M. Arabei [a], J.-P. Galaup [b,*], K.N. Solovyov [a], V.F. Donyagina [c]

[a] Institute of Molecular and Atomic Physics, NAS of Belarus, 70 F. Skaryna Ave., 220072 Minsk, Belarus
[b] Laboratoire Aimé Cotton, Bât. 505, Centre d'Orsay, 91405 Orsay Cedex, France
[c] Organic Intermediates and Dyes Institute, 1/4 B. Sadovaya Str., 103787 Moscow, Russia

Received 4 August 2004; accepted 27 October 2004

Abstract

Spectral-luminescent investigations of free-base unsubstituted 2,3-naphthalocyanine (2,3-NcH_2) in naphthalene and tetrakis(*tert*-butyl)-derivative of 2,3-NcH_2 in various solvents at room temperature, 77 and 6 K have been carried out. An essential dependence of the S_2–S_1 energy interval of the compounds investigated, $\Delta E_{S_2S_1}$, on the nature of the matrix environment has been found (the values of $\Delta E_{S_2S_1}$ lie within the limits 100 and 300 cm^{-1}). At 6 K the fluorescence spectrum of 2,3-NcH_2 has a well-resolved vibrational structure under broadband excitation, resulting practically from the emission arising from two main sites and therefore consisting of "doublets" of narrow lines. The qualitative analysis of the vibrational structure of the fine-structure fluorescence spectra of 2,3-NcH_2 enabled assessment of the form of active modes. For the two main sites efficient NH photoisomerization of the 2,3-NcH_2 molecules under selective laser excitation has been established.

1. Introduction

The methods of fine-structure vibronic spectroscopy that are based on the formation of a limited number of sites in crystalline matrices (e.g., the method of Shpol'skii spectra) possess two advantages over the methods based on removing the influence of the inhomogeneous broadening with monochromatic light (hole burning and fluorescence line narrowing). First, they enable direct investigation of transitions involving upper excited electronic states. Second, when studying phototransformation of impurity centers, it is possible to determine spectral characteristics of the photoproduct for each site.

It was of interest to apply such an approach to free-base unsubstituted 2,3-naphthalocyanine (2,3-NcH_2) having an intense longest-wavelength absorption band in the practically important spectral range about 800 nm. In [1–5], for solubilized derivatives of 2,3-NcH_2 in polymeric matrices, persistent spectral hole burning (PSHB) in the contour of the longest-wavelength absorption band was investigated, and it was shown that such materials are promising for spectral holographic recording of information with the use of ultrashort light pulses from titanium–sapphire laser.

As analysis of the literature (see, e.g., the reviews [6,7]) shows the data on spectral and photophysical properties of 2,3-NcH_2 are rather limited, which is partially connected with its extremely low solubility in organic solvents. Data are published on the position of the main absorption bands of 2,3-NcH_2 in α-chloronaphthalene [8] and in the solid state (thin film) [9]. As far as we know, information about its fluorescence is absent. The data on vibrational states were acquired by the IR spectra [9,10] and Raman (resonance Raman (RR), SERRS) spectra [10].

* Corresponding author. Tel.: +33 1 6935 2059; fax: +33 1 6935 2100.
E-mail address: jean-pierre.galaup@lac.u-psud.fr (J.-P. Galaup).

0301-0104/$ - see front matter © 2004 Elsevier B.V. All rights reserved.
doi:10.1016/j.chemphys.2004.10.045

The properties of soluble derivatives of 2,3-NcH_2, containing *tert*-butyl, alkoxy and other bulky groups, and especially those of the corresponding metal complexes, have been studied in more detail. As is known for phthalocyanines, the introduction of such groups does not essentially influence the character of the electronic absorption spectrum. The absorption spectra (or the maxima of the absorption bands) of the tetrakis(*tert*-butyl)-derivative of 2,3-NcH_2((6-*t*-Bu)$_4$-2,3-NcH_2) in various solvents and polymeric matrices are presented in [1,9,11,12]. Data on the fluorescence of (6-*t*-Bu)$_4$-2,3-NcH_2 in tetrahydrofuran are published [13] ($\lambda_{max} = 781$ nm, $\tau_F = 3.17$ ns, $\phi 1_F = 0.14$). As mentioned above, the method of PSHB at low-temperatures (several K) was applied to this compound [1–5]. Data are available about the position of the absorption bands [14,15] and the quantum efficiency of PSHB [1] for the free bases of octaalkoxy-substituted 2,3-NcH_2 which, as well as (6-*t*-Bu)$_4$-2,3-NcH_2, are easily soluble in many solvents. The IR spectrum of (6-*t*-Bu)$_4$-2,3-NcH_2 is given in the review [6].

It should be noted that, in spite of the presence of bulky *tert*-butyl-groups, the molecules of (6-*t*-Bu)$_4$-2,3-NcH_2 are prone to aggregation on increasing the concentration of the pigment in solution and on lowering its temperature [1,16,17] which is essential for experimental techniques. A conclusion that in toluene it forms trimers was drawn [16,17]. It was shown that the tendency to aggregation increases on addition of four bromine atoms to a *tert*-butyl-substituted 2,3-NcH_2, viz., for (5-Br-7-*t*-Bu)$_4$-2,3-NcH_2 [18].

The spectroscopic distinction of 2,3-NcH_2 and its derivatives is the proximity of the S_1 and S_2 (Q_1 and Q_2) electronic levels, which leads to the similarity of the absorption spectra of free bases and metal complexes. The lowering of the S_2–S_1 interval in the series: tetraazaporphin–phthalocyanine (PcH_2)–2,3-NcH_2 is obtained in quantum-chemical calculations as well [19–21]. For instance, the calculation [21] (quoted from [6]) gave the following values of this interval in the given series: 1670–710–190 cm^{-1}. In [12] the experimental value of this interval for (6-*t*-Bu)$_4$-2,3-NcH_2 is given as 243 cm^{-1} (in low-density polyethylene at 10 K). The fact of proximity of the S_1 and S_2 levels may exert a specific effect on the photoinduced NH-tautomerization process that should predominate in the PSHB in this case.

Our attempts to obtain the Shpol'skii spectra of 2,3-NcH_2 were unsuccessful due to its insolubility in *n*-alkanes and other circumstances (see below). However, it was found that 2,3-NcH_2 introduced in the naphthalene matrix by dissolving the pigment in the naphthalene melt with subsequent cooling manifests a fine-structure fluorescence spectrum at 77 K and broadband excitation. In the present work the spectral characteristics of this system and the processes of NH-phototautomerization have been investigated in detail at 6 K. The results are presented in this communication. Some results obtained for (6-*t*-Bu)$_4$-2,3-NcH_2 at 77 K and room temperature in *n*-octane and silicate gel-matrix of tetraethoxysilane (TEOS) are also included.

2. Experimental details

2,3-NcH_2 has been prepared by the demetallation of the corresponding magnesium complex in concentrated sulfuric acid. 2,3-NcMg was synthesized by the interaction of 2,3-dicyanonaphthalene [8] with magnesium in boiling α-chloronaphthalene. The purification of the complex was carried out by extraction of by-products by hot benzene and ethanol to the attainment of correspondence of the electronic absorption spectrum to that presented in the literature [22].

The synthesis of (6-*t*-Bu)$_4$-2,3-NcH_2 was performed by cyclotetramerization of 6-*tert*-butyl-2,3-dicyanonaphthalene [23] in the presence of 1,8-diazabicyclo[5.4.0]-7-undecene in boiling amyl alcohol, the product being purified by column chromatography.

The chemical structure of the compounds investigated is shown in Fig. 1. Organic solvents used in the work (*n*-octane, ethanol, chloroform, α-chloronaphthalene), as well as TEOS, were preliminarily purified by single or repeated distillation. Naphthalene of spectroscopic purity grade (''Chemapol'') was used without further purification.

Fine-structure spectra and photochemical properties of 2,3-NcH_2 were investigated in the solid matrix of unsubstituted naphthalene (at $T < 300$ K). The pigment was introduced into this matrix by dissolving the substance in molten naphthalene at $t > 80$ °C. The hot solution was poured into an optical cell of 2 mm thickness and left to cool. The obtained samples were partially transparent (weakly scattering light).

Attempts to use α-chloronaphthalene solution of 2,3-NcH_2 as an addition to *n*-octane were unsuccessful – Shpol'skii spectra could not be obtained because on diluting the α-chloronaphthalene solution by *n*-octane the solute precipitated out. Still, very weak dissolution of 2,3-NcH_2 in *n*-octane was achieved by mixing hot ($t > l80$ °C) *n*-octane with a small amount of molten naphthalene solution of the pigment. Such technique made it possible only to detect the origin of the quasiline fluorescence spectrum of 2,3-NcH_2 in *n*-octane (see Fig. 2, curve 4).

TEOS ($Si(OC_2H_5)_4$) precursor was used for inorganic silicate host. Liquid TEOS was added to water–ethanolic mixture in molar proportion TEOS–ethanol–water (1:5:5). Subsequently the reaction mixture was subjected to well-known procedures of sol–gel synthesis – 2 step inorganic polymerization (hydrolysis, then condensation) [24,25]. After the gel formation, densification was achieved by drying the gel under ambient conditions,

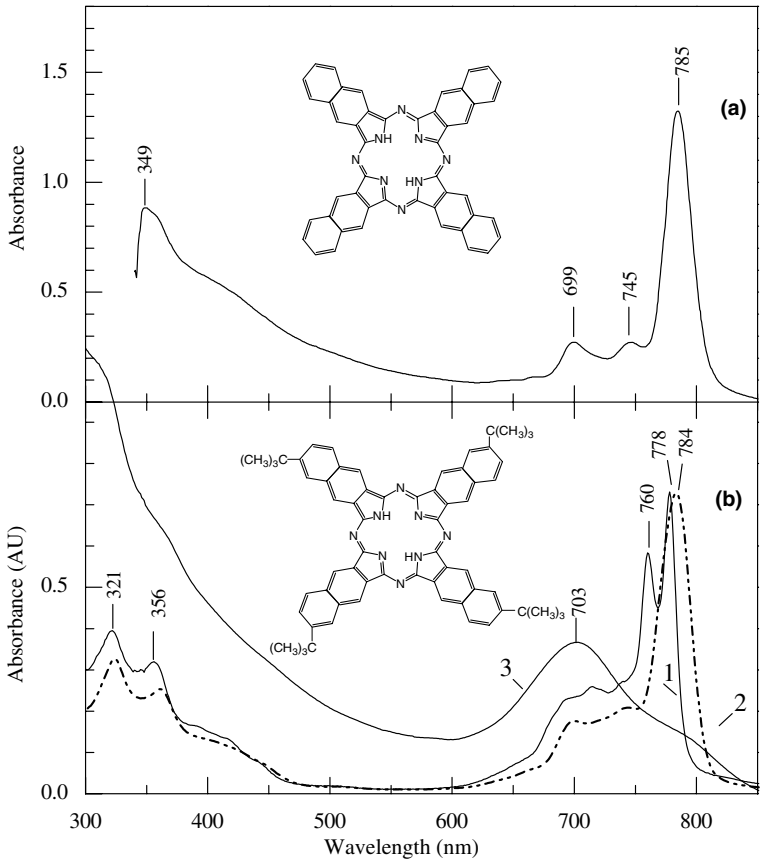

Fig. 1. Absorption spectra of 2,3-NcH_2 (a) in α-chloronaphthalene and (6-*t*-Bu)$_4$-2,3-NcH_2 (b) in *n*-octane (1), $CHCl_3$ (2) and in TEOS xerogel matrix (3) at 300 K.

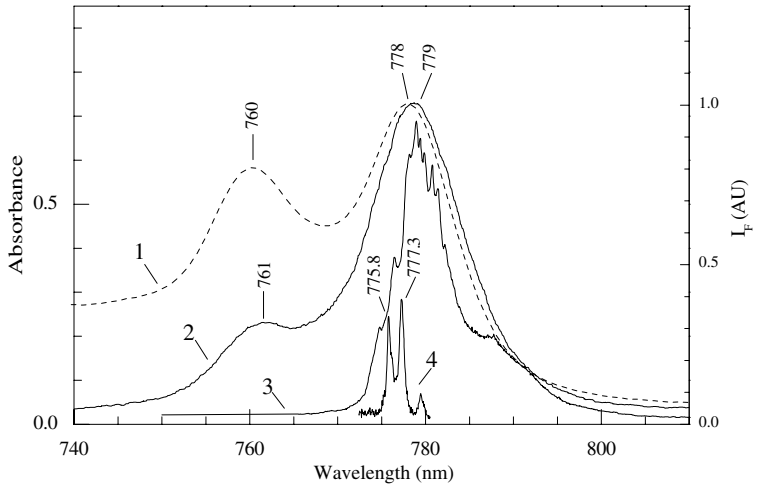

Fig. 2. Absorption (1) and fluorescence (2,3,4) spectra of (6-*t*-Bu)$_4$-2,3-NcH_2 (1,2,3) and of 2,3-NcH_2 (4) in *n*-octane at 300 K (1,2) and 77 K (3,4).

which was followed by heat treatment at 600 °C. Doping was made by impregnation in $CHCl_3$ solution of the (6-*t*-Bu)$_4$-2,3-NcH_2 pigment with subsequent drying of the sample at room temperature. Due to insolubility of 2,3-NcH2 in volatile solvents it proved impossible to incorporate it into the TEOS matrix.

The room temperature absorption spectra were measured using a Cary 400 Scan spectrophotometer from Varian. At low temperatures the absorption spectra of the samples were measured as transmission spectra. For this purpose a HRP 600 Jobin Yvon monochromator (inverse linear dispersion 1.2 nm/mm) was used, with

the help of which the spectral attenuation of the intensity of white light from a stabilized incandescent lamp transmitted by the sample was monitored. The absorbance (A) at the maximum of the longest wavelength absorption band was ~0.2 for 2,3-NcH_2 in naphthalene (sample thickness $l = 2$ mm) and ~0.7 for solution of (6-*t*-Bu)$_4$-2,3-NcH_2 in *n*-octane ($l = 10$ mm) which corresponds to concentrations less than 10^{-5} M/l.

The fluorescence spectra of 2,3-NcH_2 in naphthalene at different temperatures, including the fine-structure spectra at 6 K, were obtained either under broadband excitation with a Xe lamp (320–650 nm), or under selective laser excitation (with a diode laser at a wavelength about 792 nm, $\Delta\nu_{laser} \approx 0{,}1$ cm^{-1}, driven with temperature and current stabilization modules). Typical total irradiation power of the diode laser (in experiments on luminescence and photo-transformations, as well) was in the range 10–15 mW, determining power density range from 40 to 60 mW cm^{-2}. The exact wavelength was determined with a Burleigh WA1100 wavemeter. The fluorescence was monitored with a red-sensitive PM (R943-02 from Hamamatsu) placed beyond the same HRP monochromator and followed with a picoammeter. The samples were positioned in an optical liquid-helium bath cryostat (SMC-L'Air Liquide).

Continuous-wave titanium–sapphire laser, tunable in the 760–800 nm range, was used for measurements of the fluorescence excitation spectra with selective monitoring of fluorescence for the 0–0 quasi-lines of individual sites of 2,3-NcH_2 in naphthalene at 6 K.

Quasi-line spectra (QLS) of fluorescence in *n*-octane at 77 K (for (6-*t*-Bu)$_4$-2,3-NcH_2 and 2,3-NcH_2), as well as room-temperature fluorescence spectra, were recorded using a spectrometric set-up assembled on the basis of two monochromators (double monochromator of inverse linear dispersion 0.8 nm/mm for monitoring) and a photon-counting detection system [26]. For the excitation of fluorescence, the light of a xenon lamp was used.

Photo-transformations of 2,3-NcH_2 were studied at 6 K with the use of monochromatic light of either the diode laser, or the titanium–sapphire laser, mainly in combination with broadband excitation (320–650 nm, from the xenon lamp). The fluorescence of individual sites was monitored selectively.

3. Results and discussion

3.1. Absorption and fluorescence spectra

The absorption spectrum of 2,3-NcH_2 in α-chloronaphthalene is shown in Fig. 1(a). As already mentioned, due to the proximity of the S_1 and S_2 (Q_1 and Q_2) levels, it is similar to the spectra of metal complexes (2,3-NcM) [6,8]. For the sake of comparison and clarification of the spectral pattern, in Fig. 1(b) we present the absorption spectra of (6-*t*-Bu)$_4$-2,3-NcH_2 in solvents which are transparent in the UV region. The visible spectrum of this pigment in chloroform (curve 2) is similar to the spectrum of 2,3-NcH_2, although some differences take place in the region of the vibronic band at 745 nm. Such similarity is not surprising since both compounds have the same conjugated π-bond system, the porphyrazine (tetraazaporphin) macrocycle extended by the addition of naphthalene rings. The spectrum in *n*-octane (curve 1), based on the totality of the evidences given above in the Introduction, is interpreted as belonging to two allowed electronic transitions $S_1 \leftarrow S_0$ ($Q_1 \leftarrow G$) and $S_2 \leftarrow S_0$ ($Q_2 \leftarrow G$) at 778 and 760 nm, respectively. The distance between the S_1 and S_2 levels is obtained as 305 cm^{-1}. In chloroform (curve 2), these transitions merge into one absorption band and, therefore, the S_2–S_1 interval in this case is much smaller, the splitting of the degenerate Q state of D_{2h} symmetry being hidden in the contour of the 0–0 band with maximum at 784 nm and half-width of ~500 cm^{-1}. Thus, the S_2–S_1 interval of this 2,3-NcH_2 derivative depends essentially on the nature of external medium.

The spectrum of (6-*t*-Bu)$_4$-2,3-NcH_2 in *n*-octane may be compared with the absorption spectrum of tetrakis (4-*tert*-butyl)phthalocyanine ((4-*t*-Bu)$_4$-PcH_2) in *n*-heptane [27]. Linear annelation of the benzene rings to the phthalocyanine chromophore results in the bathochromic shift of the two main bands in the red region (by ~1500 cm^{-1} for the longest-wavelength band) and in the decrease in the S_2–S_1 interval (for (4-*t*-Bu)$_4$-PcH_2 it is equal to ~1300 cm^{-1}). In the UV region the two bands of (6-*t*-Bu)$_4$-2,3-NcH_2 at 321 and 356 nm, presumably, correspond to the band of (4-*t*-Bu)$_4$-PcH_2 at about 350 nm. This band at 350 nm shows evidence of splitting into two components, although it cannot be excluded that the 321 nm band may belong to the naphthalene fragments. In the 400–450 nm range, an appreciable intensification of the absorption is observed for (6-*t*-Bu)$_4$-2,3-NcH_2.

It is appropriate to note here that the effect of naphtho-substitution on the electronic structure, electronic spectra, and photophysics of molecules of porphin and its derivatives was subjected to complex experimental and theoretical investigation in [28]. It should be noted that naphtho-substitution in the porphyrin macrocycle may be considered as the fusion of additional benzene rings to the molecule of a benzoporphyrin, e.g., tetrabenzoporphyrin ($TBPH_2$), analogously to the change from phthalocyanine to naphthalocyanine. Quantum-chemical calculation (PPP) [28,29] showed that the experimentally observed bathochromic shift of the Q bands on the annelation of additional benzene rings to the $TBPH_2$ molecule is caused by the energy rise of the highest occupied MO (HOMO) of the a_{1u} type due

to its delocalization over the extended conjugated π-bond *system*. [1] Moreover, the reason was established of greater bathochromic shift of the Q band for Zn-2,3-tetranaphthoporphin than for Zn-1,2-tetranaphthoporphin and of other differences between linear and angular annelation of additional benzene rings: linear annelation extends the conjugated π-bond system more effectively. Such calculations were carried out for quite a number of porphin derivatives with annelated aromatic nuclei: naphthalene, anthracene, and phenanthrene, both for metal complexes (without explicit account of the metal atom) and free bases [29]. Later, theoretical analysis of the effect of benzene rings annelation on the electronic properties of the phthalocyanine macrocycle was carried out [19–21]. In particular, it was shown [19] that for 2,3-NcH_2 the $6a_u$ HOMO increases its energy by 0.39 eV relatively to the related $4a_u$ HOMO of PcH_2 which leads to a considerable red shift of the longest-wavelength transitions ($6a_u \rightarrow 8b^*_{3g}, 8b^*_{2g}$).

Free-base 2,3-$TNPH_2$ (tetra-napthoporphyrin) could not be isolated due to its instability. However, Kopranenkov et al. succeeded in preparing *meso*-phenyl substituted 2,3-$TNPH_2$ [30], as well as *meso*-phenyl substituted 2,3-tetraphenanthroporphin whose photophysics has been investigated experimentally [31]. In agreement with quantum-chemical calculations for the corresponding chromophores without *meso*-phenyl substitutions [29], the absorption spectra of the two compounds in the Q bands region are similar. They show that the S_2–S_1 interval is decreased relatively to $TBPH_2$ and amounts to ~450 and ~500 cm^{-1}, respectively, i.e., it is nevertheless larger than for 2,3-NcH_2.

The results of quantum-chemical calculations [28] give an explanation of the appearance of absorption in the 400–450 nm region of the absorption spectrum of 2,3-NcH_2 (see above). The calculations show that in this region electronic transitions appear that correspond to intramolecular charge (electron density) transfer from the inner 16-membered ring to the naphthalene fragments.

The absorption spectrum of (6-*t*-Bu)$_4$-2,3-NcH_2 incorporated into the TEOS matrix is given in Fig. 1(b) (curve 3). One can see that the characteristic structure of the Q bands has disappeared although absorption in the red is retained. We interpret this spectrum as belonging to aggregates formed inside the nanopores of TEOS. It has to be noted that an analogous behavior of the absorption spectrum was observed also for toluene solution of (6-*t*-Bu)$_4$-2,3-NcH_2 [16] where the band at 700 nm attributed to aggregate formation increased in intensity with increasing the concentration of the pigment.

We turn now to emission spectra. Fig. 2 shows the fluorescence spectra of (6-*t*-Bu)$_4$-2,3-NcH_2 in *n*-octane at room and liquid nitrogen temperatures (curves 2 and 3). As seen in the fluorescence spectrum at 300 K, a band at 761 nm is observed. This band completely disappears on lowering the temperature. Evidently, this band belongs to the $S_2 \rightarrow S_0$ fluorescence, which is enabled by the thermal population of the S_2 level. At 77 K the 0–0 band is narrower and displays features of quasi-line structure. The complexity of the origin "multiplet" of this QLS may be caused by two reasons: (1) the presence of bulky *tert*-butyl groups increases the number of sites in the *n*-alkane matrix; (2) 0–0 quasi-lines of different randomers may have different wavelengths (randomers are position isomers differing in the mutual disposition of side substituents of fragments of a complex molecule).

An analogous partially resolved fluorescence QLS of (6-*t*-Bu)$_4$-2,3-NcH_2 has been obtained in *n*-decane. On the contrary, spectra in *n*-hexane and *n*-nonane are diffuse, which is indicative of differences in the crystal structure of these two groups of *n*-alkanes.

The fluorescence spectrum of 2,3-NcH_2 in α-chloronaphthalene could not be recorded, neither at 300 K, nor at 77 K, due to efficient photo-destruction of the pigment under the action of the exciting light.

Fortunately, we have found, as already mentioned, that solidified solution of 2,3-NcH_2 in molten naphthalene exhibits normal molecular fluorescence. The absorption and fluorescence spectra of this system at 300 K are shown in Fig. 3. The absorption spectrum of 2,3-NcH_2 in naphthalene (curve 1) is close to that in α-chloronaphthalene (cf. Fig. 1(a)), but the Q band is evidently split into two components with frequency difference of 120 cm^{-1}. Analogously to (6-*t*-Bu)$_4$-2,3-NcH_2 in *n*-octane, the fluorescence spectrum of 2,3-NcH_2 in naphthalene contains the S_2S_0 component; however, due to close overlap with the $S_1 \rightarrow S_0$ fluorescence, it is revealed only by mathematical treatment (decomposition) of the contour of the 0–0 band of the fluorescence spectrum.

Preliminary experiments showed that lowering the temperature down to 77 K, under broadband excitation, resulted in the resolution of the 0–0 band of the $S_1 \rightarrow S_0$ fluorescence spectrum into a complex origin "multiplet" with two main components separated by $\Delta\nu = 42$ cm^{-1} (see Fig. 4(a), curve 3). Vibronic satellites accompanied them, so that fine-structure fluorescence spectrum arose.

We also attempted to introduce 2,3-NcH_2 into an *n*-octane matrix by pouring together hot *n*-octane and the solution of the pigment in naphthalene melt with subsequent immediate freezing in liquid nitrogen. The concentration of fluorescent impurity centers of 2,3-NcH_2 in the sample was extremely low, so that we only

[1] Unfortunately, the characteristics of the boundary MOs are not given in the text of [28]. The energy rise of the porphin HOMO due to its interaction with the naphthalene MOs is noted in [29].

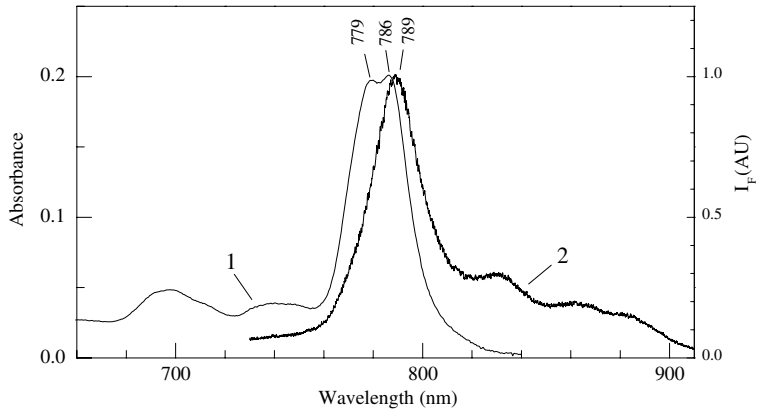

Fig. 3. Absorption (1) and fluorescence (2) spectra of 2,3-NcH_2 in naphthalene at 300 K.

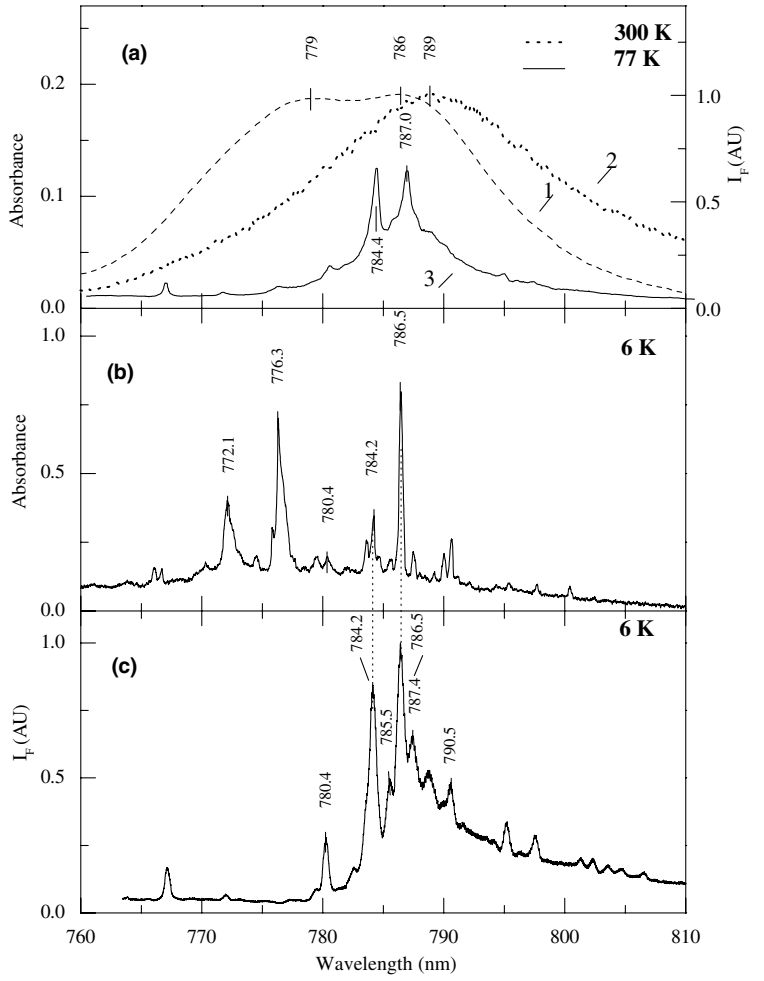

Fig. 4. Absorption (a1,b) and fluorescence (a2,a3,c) spectra of 2,3-NcH_2 in naphthalene at 300 K (a1,a2), 77 K (a3) and 6 K (b,c).

could detect the origin "multiplet" of the fluorescence QLS, which is shown in Fig. 2, curve 4. It is seen that the "multiplet" also has two main components. This "doublet" has $\Delta\nu = 25$ cm^{-1} and it is shifted by $\sim$9 nm ($\sim$150 cm^{-1}) to the blue relatively to that one observed in naphthalene, which is indicative of a stronger guest–host interaction in the naphthalene matrix.

The appearance of the fine-structure fluorescence spectrum of 2,3-NcH_2 in naphthalene at 77 K means that the pigment forms a limited number of types of impurity centers (sites) in this matrix and that their 0–0 and vibronic bands are broadened homogeneously, their width depending strongly on temperature. One could expect that further lowering of the temperature

down to that of liquid helium would give fine-structure spectra of much higher quality. Our experiments proved this to be the case.

The results of our spectroscopic investigations at 6 K are presented in Figs. 4(b) and (c) and 5. In Fig. 4(a) curves 1 and 2 are fragments of curves 1 and 2 of Fig. 3, but on a different (expanded) wavelength scale.

Fig. 4(c) shows that, as expected, at 6 K the resolution in the fluorescence spectrum, recorded also under broadband excitation, is much better than at 77 K. One can see that in the region from 765 to 800 nm there are several lines, which may be attributed to different sites. Some of them, however, may be vibronic satellites. The vibrational structure of the spectra depicted in Fig. 5 is analyzed in Section 3.2. Here, we note only that the vibronic fine-structure spectra are essentially "doublet" in character. This means that the intensities of the origin "doublet" lines in Fig. 4(c) are underestimated, possibly due to reabsorption.

The absorption spectrum of 2,3-NcH_2 in naphthalene at 6 K was obtained too. The juxtaposition of the absorption and fluorescence spectra shows that the position of a number of peaks exactly coincides, in particular, for the main "doublet" components. These lines evidently belong to the 0–0 transitions $S_1 \leftarrow S_0$ of different sites. The establishment of correlations of these transitions with the $S_2 \leftarrow S_0$ transitions and vibronic transitions in absorption required measurements of fluorescence excitation spectra for individual sites.

Such measurements have been performed. Although the obtained excitation spectra are not of good quality (both for technical reasons and in connection with NH-phototautomerism described in Section 3.3), they made it possible to fully decipher the spectral patterns presented in Figs. 4(b) and (c). The results of the analysis of the origin "multiplet" region are as follows.

The fluorescence lines at 780.4, 784.2, 785.5, 786.5, 787.4, and 790.5 nm belong to separate sites and find exact correspondence in the absorption spectrum (we neglect very weak lines in both spectra). Thus, the span of the origin "multiplet" of the system under study is ca. 200 cm^{-1}, which is larger than what is usually observed in *n*-alkane matrices (less than 100 cm^{-1}).

The measurements of fluorescence excitation spectra have shown that the 772.1 and 776.3 nm bands belong to the impurity centers having the $S_1 \leftarrow S_0$ 0–0 transition at 784.2 nm, i.e. they are associated with the short wavelength component of the origin "doublet". We interpret the appearance of these bands as the result of the vibronic interaction of the S_2 level with vibrational sublevels of the S_1 state. Such splitting of the $S_2 \leftarrow S_0$ transition (vibronic analogue of Fermi resonance in Herzberg's terminology [32]) was noted for the long-wavelength site of PcH_2 [33]; the vibronic interaction is more complicated for PcD_2 and phthalocyanine-d_{16} [34] as well as for tetraazaporphin [35,36]. In our case the vibronic interaction is also complicated since, as seen from Fig. 4(b), the 772.1 and 776.3 nm bands are

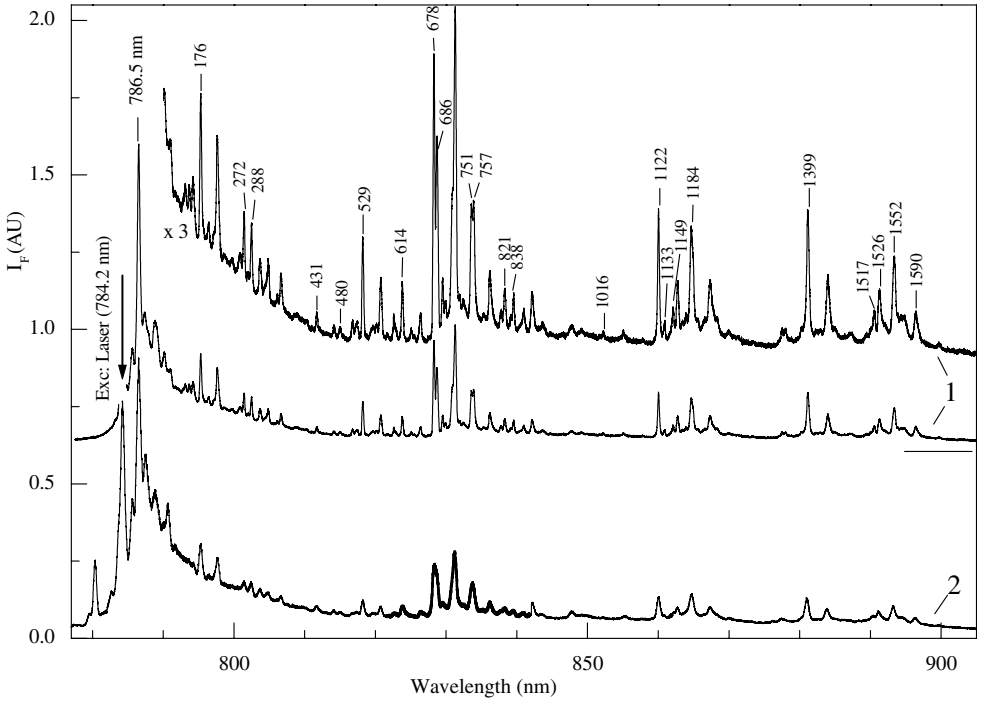

Fig. 5. Fluorescence spectra of 2,3-NcH_2 in naphthalene at 6 K. Excitation: diode laser ($\lambda_{exc} = 784.2$ nm) (1) and xenon lamp (broadband excitation in the 320–650 nm region) (2). On curve 1 the values of the normal mode frequencies (in cm^{-1}) are indicated for the "blue" centers.

structured. Neglecting their structure, by using the mean frequency of these bands one can estimate the S_2–S_1 interval for the short-wavelength site and, correspondingly, the frequency of the main active non-totally symmetrical vibration as 165 cm^{-1}.

For the long-wavelength site having the origin line at 786.5 nm the excitation spectrum is different. It shows that a weak line at 778.6 nm should be assigned to the $S_2 \leftarrow S_0$ 0–0 transition. Elucidation of the cause of the low intensity of the $S_2 \leftarrow S_0$ transition in this case will require additional investigations.

From Fig. 4, it is seen that the intensity ratio in the origin "doublet" of the fluorescence spectrum of 2,3-NcH_2 in naphthalene does not correspond to that in the absorption spectrum. The reason of this is that under steady-state conditions of excitation of a system of centers capable of photoinduced interconversion dynamic equilibrium is established and the intensity ratio for emission of different centers is determined only by the relation between the rate constants of the photoprocesses [37,38], and not by the initial concentration of centers which is reflected in the absorption spectrum.

3.2. Vibrational structure of the fluorescence spectrum

As it may be seen from Fig. 5 (curve 2), the obtained fine-structure spectrum of 2,3-NcH_2 in naphthalene under broadband excitation is of good quality, which allows the determination of vibrational frequencies in the ground S_0 state and of the activity of the normal modes. Fig. 5 (curve 1) shows that still better spectral resolution is achieved under the selective laser excitation of the short-wavelength site. It should be emphasized that this improvement of the spectrum is not accompanied by the disappearance of some lines. Since under the selective laser excitation involving only the two main sites (see below), the other sites are not excited, this means that the vibronic lines of fluorescence of these minor sites are weak under broadband excitation. This statement was made in Section 3.1, based on the "doublet" character of the fluorescence spectrum of Fig. 5 (curve 1). Evidently, it finds corroboration in the results of the experiments with laser excitation.

It would be preferable to obtain the fluorescence spectrum under selective excitation of the long-wavelength site. However, the NH-photoisomerization in the centers of this type leading to their transformation into the short-wavelength site resulted to be so fast that it was impossible to record the spectrum. Under selective excitation of the short-wavelength site, evidently, the short-wavelength centers are also transformed into the long-wavelength ones, but the latter are excited to, via the phonon sidebands in absorption, and eventually a dynamic equilibrium is established. Somewhat surprising is that the intensity ratio in the "doublets" of Fig. 5 (curves 1 and 2) is almost the same. The photochemical aspects are considered in more detail in Section 3.3.

The results of vibrational analysis of the fine-structure fluorescence spectra of 2,3-NcH_2 are presented in Table 1. For comparison frequencies from the RR spec-

Table 1
Correlation of vibrational frequencies (in cm^{-1}) from the fine-structure fluorescence spectrum of 2,3-NcH_2 with those from the RR spectrum and from the fluorescence QLS of PcH_2

2,3-NcH_2		PcH_2	Tentative assignment[b] for 2,3-NcH_2
Fluorescence (naphthalene)	RR[a] (KBr) [10]	Fluorescence (*n*-alkanes) [44]	
176	171	184	
272			
288	285		
431			
480	478	488	Isoindole SD
529	528	546[c]	Isoindole (SD + SB)
	559*		
614	611		Naphthalene SD
678	679	684	(aza + isoindole) SD
686		726[c]	Pyrrole SD + aza str.
720	717		Naphthalene SD
751			Naphthalene SD
757	757	801[c]	Aza SD + benzene SB
821	819		Naphthalene NA
838	835	837	Benzene SB
875[d]	894	888	Naphthalene SB
	914*	945[e]	Aza (SD + str.)
	971*		
1016	1015	1028	Pyrrole SB (CN)
	1050*		
	1096*		
1122	1120	1120[e]	δCH + benzene str.
1133	1132		Naphthalene δCH
1149	1149	1143	Pyrrole (SB + SD)
	1164*		
1184	1180	1180	δCH
	1309	1318[f]	δCH + benzene str.
1336	1352	1348	(see text)
	1366*		Naphthalene str.
1399	1394		(see text)
	1409*	1404[f]	Isoindole str.
	1422	1421[e,f]	Isoindole str.
1434	1437	1455	Aza str.
1517	1512	1495	Benzene str. + δCH
1526		1517	Aza str.
	1540		
1552		1555	Aza str. + pyrrole (str. + SD)
1590	1598*		Naphthalene str.
	1627	1624	Naphthalene str.

[a] The exciting light wavelength $\lambda_{exc} = 647.1$ nm. Frequencies from the spectrum obtained at $\lambda_{exc} = 514.5$ nm are marked by an asterisk.

[b] *Abbreviations*: SD, skeletal distortion; SB, skeletal breathing; str., stretching; δCH, in-plane CH bending; NA, not assigned in [39].

[c] Correlation with the corresponding frequencies of 2,3-NcH_2 is questionable.

[d] The appearance of this frequency in the spectrum is uncertain.

[e] Observed only for PcZn (RR) [47].

[f] The frequency finds correspondence only in the RR spectra of 2,3-NcH_2.

tra [10] are also given. It is seen from Table 1 that the frequency values obtained from different spectra are in good agreement. Some frequencies are absent in the fluorescence spectrum, whereas some frequencies are not observed in the RR spectra. Pairs of frequencies 678 and 686 cm^{-1}, 751 and 757 cm^{-1}, and 1526 and 1552 cm^{-1} correspond to single frequencies in the RR spectra indicating their accidental degeneracy. As usual, the data obtained by the two methods complement each other mutually.

It is impossible to determine the form of the normal modes that are active in the 2,3-NcH_2 spectra without a normal coordinate analysis. Tentative assignment of a number of vibrational frequencies of 2,3-NcH_2 was proposed in [10] on the basis of literature data on qualitative analysis of vibrational spectra of naphthalene [39,40] and PcH_2 [41–43]. An evaluation of the results of this analysis is given below. Our approach to the qualitative analysis of the fluorescence and RR spectra of 2,3-NcH_2 is somewhat different. In the third column of the Table 1, we list those vibrational frequencies from the vibronic QLS of PcH_2 [44] (17 of 25 observed) that are close to the frequencies obtained from our fine-structure fluorescence spectrum of 2,3-NcH_2 (first column in the Table 1). It should be noted that the data of the early work by Personov [44], where photographic technique was used, are in good agreement with the newer work [45] in which α-chloronaphthalene was used as a dissolving additive. The PcH_2 frequencies are correlated with the frequencies of in-plane even vibrations of PcZn for which data are available on the effect of perdeuteration (PcZn-d_{16}) on the IR spectra [46] and RR spectra [47] and classical normal coordinate analysis was carried out [46,47] as well as the quantum-chemical calculation of the normal modes [48]. On this basis for the selected frequencies of PcH_2 the form of the modes has been assessed by analogy with PcZn [47,48], and this assessment has been transferred on 2,3-NcH_2 (presented in the fourth column of the Table 1).

The frequencies of 2,3-NcH_2, which are absent in the fluorescence QLS of PcH_2, may belong to the naphthalene fragments. A comparison of these frequencies with the data for naphthalene [39,40] shows that 10 frequencies may be assigned to naphthalene vibrations, including four modes with predominant CH character. Two frequencies, which appear only in the RR spectra: 1309 and 1366 cm^{-1} may be added to them. It should be noted that the large contribution of δCH deformations to the modes of PcZn that are related to those of 2,3-NcH_2 having frequencies of 1188, 1318, and also 1495 cm^{-1} is proven by the data on perdeuteration effect on the RR spectra [47].

The assignment of the 1336 and 1399 cm^{-1} fluorescence lines requires special consideration. In this region naphthalene has four vibrational frequencies: 1339, 1360, and 1387 cm^{-1} (IR) and 1376 cm^{-1} (Raman). One of them should correlate with the mentioned above 1366 cm^{-1} frequency of 2,3-NcH_2. In the fluorescence QLS of PcH_2 the 1348 cm^{-1} quasi-line is strong. Proceeding from the frequency closeness considerations, one might correlate the 1336 cm^{-1} frequency of 2,3-NcH_2 (1352 cm^{-1} in RR) with the 1348 cm^{-1} frequency of PcH_2. However, the form of the 1348 cm^{-1} mode of PcH_2 is such (judging from the data on PcZn [47]) that it should be retained in passing from PcH_2 to 2,3-NcH_2; therefore, high intensity of the corresponding vibronic transition is to be expected, whereas the 1336 cm^{-1} line is weak. Based on intensity considerations, the 1399 cm^{-1} line of 2,3-NcH_2 should correspond to 1348 cm^{-1} line of PcH_2, but the frequency difference seems to be too large. Hence, we believe that in this region quantum-mechanical interaction of the type of Fermi resonance takes place between the modes of the macrocycle and naphthalene fragments, the high-frequency component gaining in vibronic intensity (however, cases of accidental degeneracy of vibrations are also possible). It follows from this discussion that at least one mode of the naphthalene fragments should be added to those 12 which were considered above.

Comparing our assignment with that of [10] we note that, apart from the naphthalene vibrations in the 1100–1650 cm^{-1} range, we agree also with the assignment of the 1409 and 1422 cm^{-1} frequencies of 2,3-NcH_2 (RR, isoindole stretching) and, partially, with that of the 1149 cm^{-1} (pyrrole, not only skeletal breathing, but also skeletal distortion) and 1540 cm^{-1} (RR, aza stretching). In the latter case, data on the RR spectra of PcZn and PcZn-d_{16} [47] helped to clarify the situation. The corresponding frequency of 1506 cm^{-1} of PcZn is accidentally degenerate; deuteration reveals two components of A_{1g} and B_{1g} symmetry (D_{4h} symmetry group). It is natural to correlate them with the 1527 and 1555 cm^{-1} frequencies of PcH_2 and, correspondingly with the 1526 and 1552 cm^{-1} frequencies of 2,3-NcH_2 (fluorescence in naphthalene). Therefore, we believe that the 1540 cm^{-1} line in the RR spectra of 2,3-NcH_2 in KBr is also a case of accidental degeneracy. Of the two mentioned vibrations of PcZn, the B_{1g} mode is almost completely localized on the aza bridges while the A_{1g} mode contains also contributions from pyrroles. It cannot be excluded that the correlation between the fluorescence and RR frequencies could be different from the one presented in the table, viz., it may be as follows: 1526–1512, 1552–1540 cm^{-1}.

We disagree with the assignment of [10] in the case of the following frequencies (numerical values from the fluorescence spectrum): 678, 757, 875, 1016, 1434, and 1517 cm^{-1}. In fact, we have proposed the interpretation of the low-frequency range of in-plane even vibrations of 2,3-NcH_2 (400–1100 cm^{-1}), as shown in Table 1.

3.3. Photoinduced NH tautomerism

One of the aims of our research was to examine the process of NH photoisomerization in the case 2,3-NcH_2. It is known that free-base porphyrins in Shpol'skii matrices form pairs of sites differing in the position of the two central imino hydrogens, so that transformation of one site into another due to synchronous displacement of protons is formally equivalent to rotation of the porphyrin molecule as a whole by $\pi/2$. Such reversible interconversion of sites is observed under selective excitation of one site by monochromatic light as was shown in [49] for $TBPH_2$ and in [33] for PcH_2 and porphin. Using narrow-band laser excitation makes it possible to burn persistent holes in the inhomogeneously broadened Shpol'skii quasi-lines (first studies of photochemical hole burning were performed for PcH_2 [50] and porphin [37]). This phenomenon of photoinduced NH-isomerization in amorphous media leads to specific time dependences of fluorescence polarization [51] and presents an efficient mechanism for PSHB in absorption bands [52].

It follows from the preceding material that the two main sites of 2,3-NcH_2 in naphthalene undergo efficient interconversion under the influence of laser light. We have carried out kinetic experiments with combined excitation to characterize the effect in more detail. Some results of this study are presented in Fig. 6.

The wavelength of the diode laser was tuned on the 0–0 transition of an individual site to ensure a selective resonance excitation of the impurity centers of the given type. Only the data for the two main sites are presented in Fig. 6. For convenience, we call the short-wavelength centers "blue" ($\lambda_{00}^{blue} = 784.2$ nm) and the long-wavelength centers "red" ($\lambda_{00}^{red} = 786.5$ nm). Changes in the number of centers of a given site were monitored by the fluorescence intensity corresponding to vibronic transitions involving vibrations of 679 and 686 cm^{-1} frequencies (cf. Fig. 5): for the "blue" centers, λ_{mon} was 828.6 nm and for the "red" ones, λ_{mon} was 831.0 nm. Sections of the time dependences of selectively monitored fluorescence at excitation by laser (only) are designated in Fig. 6 by L. Sections corresponding to non-selective Xe lamp light excitation (320–650 nm range) are designated by X, and those corresponding to combined excitation, by LX.

Fig. 6(a) demonstrates the behavior of the intensity of fluorescence of the "red" centers, i.e., of their concentration under different excitation regimes. It is seen that, after cessation of the non-selective excitation and a dark pause, at the onset of the laser excitation, the fluorescence intensity grows up immediately and exceeds by three times its value under non-selective excitation, but also, it falls down abruptly, on a time scale of a fraction of second (so that the kinetics may be called a spike), and then decreases below its value for non-selective excitation, as a result of a slower process. The addition of the non-selective excitation to the selective laser radiation leads to a considerable increase in the intensity of fluorescence of the "red" centers.

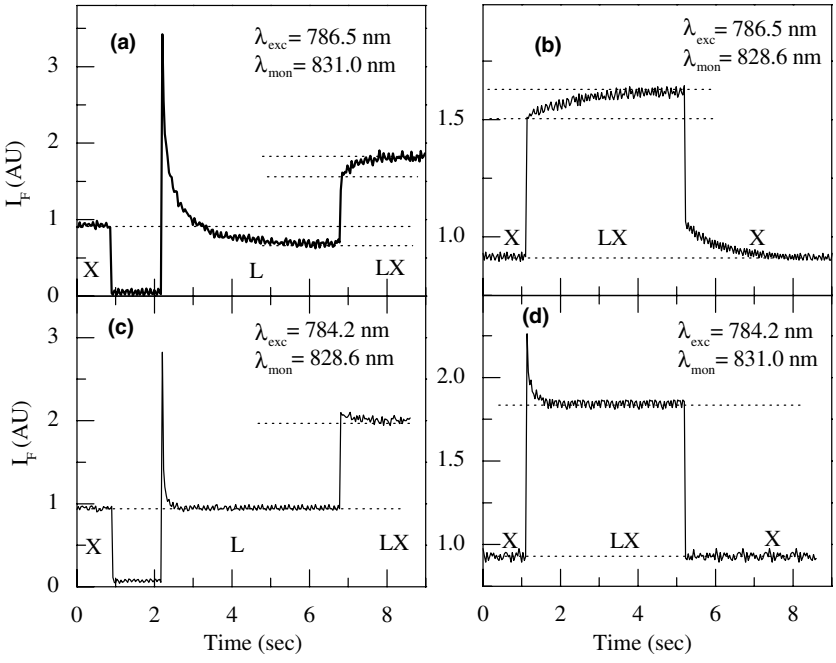

Fig. 6. Time dependences of the fluorescence intensities of individual sites ($\lambda_{mon} = 828.6$ and 831.0 nm) of 2,3-NcH_2 in naphthalene at 6 K after changing the regime of excitation (X denotes the xenon lamp excitation; L, the laser excitation (λ_{exc} is indicated); LX, the combined laser and lamp excitations).

We interpret these data in the following way. Under non-selective excitation, a dynamic equilibrium between photoinduced transformations "blue" ↔ "red" is established as noted in Section 3.1, and steady-state concentrations of "blue" and "red" centers are achieved. They are conserved during the dark pause (at 6 K). The selective laser excitation of the "red" centers gives high value of the fluorescence intensity, but as the result of efficient phototransformation, their concentration drops sharply. The existence of the slow phase of this process seems to be associated with inhomogeneity of the centers. The addition of a non-selective excitation to the laser light (LX) leads again to a dynamic equilibrium, the "red" centers concentration being increased. Though its steady-state value should be lower than without laser light, the increased power due to the combined excitation compensates this effect, and the fluorescence intensity is high. The presence of slow kinetics in section LX is connected with the establishment of a dynamic equilibrium.

By a qualitative estimate, the photoisomerization kinetics for the "red" site appears to be neither exponential, nor even bi-exponential (Fig. 6(a)). A similarly stretched kinetics was observed earlier, e.g. for spectral hole-burning of substituted tetraazaporphin in a Langmuir–Blodgett film [53,54]. It is caused mainly by the inhomogeneity of impurity centers (in height and spatial width of barriers of tunneling processes); for randomly oriented centers the effect of excitation anisotropy should also be considered [55]. We infer from the burning kinetics under consideration that the fluorescence and absorption 0–0 lines (origin "doublet") are broadened inhomogeneously, the centers of almost equal 0–0 frequency differing in tunneling parameters. For a crystal matrix it is somewhat surprising, but it must be borne in mind that our samples were not prepared under equilibrium conditions.

In Fig. 6(b) the behavior of the "blue" centers under the excitation of the "red" ones is shown. The addition of the selective laser excitation of the "red" centers to the non-selective excitation results in a considerable increase of the fluorescence intensity of the "blue" centers that is indicative of the increase of their concentration.

Figs. 6(c) and (d) are analogous to Figs. 6(a) and (b) in the manner of the variation of the excitation conditions, but under the excitation of the "blue" centers. Fig. 6(c) corresponds to Fig. 6(a) – the fluorescence is monitored for those centers, which are excited. Under the excitation of "blue" centers, the difference is that they are not burned out completely, but the dynamic equilibrium between "blue" and "red" centers is created, due to the excitation of the latter via their phonon sidebands as discussed above (see Section 3.1). A comparison of Fig. 6(c) with Fig. 6(a) shows that this process proceeds much faster than the burning-out of the "red" centers, and in the most part of section L the value of I_F is constant. In the section LX the steady-state value of I_F is reached with roughly the same rate.

Fig. 6(d) corresponds to Fig. 6(b) since the fluorescence is monitored not for the centers that are selectively excited, but for those that are formed. According to the data of Fig. 6(d), in this case the steady-state values of I_F in the sections X and LX are reached also fast. A relatively small spike in the LX section is explained by the fact that in the detected fluorescence line 831.0 nm there is a component belonging to "blue" centers ($\nu_{00}^{blue} = 720$ cm^{-1}, see Table 1 and Fig. 5).

Thus, the obtained experimental data confirm our conclusion that "blue" and "red" centers are capable of reversible photoinduced interconversion which is characteristic of the NH phototautomerism in free-base porphyrins. In other words, the results of experiments performed manifest efficient NH phototautomerism in 2,3-NcH_2 in the naphthalene matrix.

4. Conclusion

The use of naphthalene as a (solid) solvent enabled us to obtain the spectral characteristics of the fluorescence of unsubstituted 2,3-NcH_2 at 300, 77, and 6 K. At room temperature for 2,3-NcH_2, as well as for (6-*t*-Bu)$_4$-2,3-NcH_2, the $S_2 \rightarrow S_0$ fluorescence due to the thermal population of the S_2 level is observed The S_2–S_1 interval is small for both molecules; at the same time, the absorption spectra show that its value essentially depends on the nature of solvent (between the limits 100 and 300 cm^{-1}).

The study carried out has shown that the 2,3-NcH_2 molecules embedded into the naphthalene matrix occupy a limited number of sites (types of impurity centers) possessing at 6 K narrow 0–0 lines assigned to the $S_1 \leftarrow S_0$ transition (in the 780–791 nm wavelength interval) whose position in the absorption and fluorescence spectra exactly coincides. On rising up the temperature, they are homogeneously broadened, so that at 77 K the structure of the 0–0 band is still noticeable, while at 300 K it has disappeared completely.

The fluorescence spectrum at 6 K under broadband excitation consists practically of "doublets" of narrow vibronic lines generated by the origin lines at 784.2 nm ("blue" centers) and at 786.5 nm ("red" centers). Under selective laser excitation of the "blue" centers, the fine-structure fluorescence spectrum of 2,3-NcH_2 is similar, but shows a higher resolution, due to the narrowing of the vibronic lines.

The selective laser excitation of the "red" centers results in their fast burning out, which does not allow the recording of a stationary fluorescence spectrum. It has been proven by kinetic measurements in a time scale of seconds that the "blue" and "red" centers are capable of photoinduced interconversion. It is inferred that this

is due to NH phototautomerism. Under broadband excitation and under the excitation of the "blue" centers, a dynamic equilibrium is established in the system; which makes possible the recording of the fluorescence spectrum.

The juxtaposition of the fine-structure vibronic spectrum of 2,3-NcH_2 with the RR spectra [10] shows good agreement of the vibrational frequencies. In some cases, the fluorescence spectrum is more informative. A qualitative analysis of the vibrational structure of the spectra has been carried out and the assignment of a number of modes has been reconsidered. It is shown that more than 12 vibrational frequencies may be ascribed to vibrations of the naphthalene fragments of the 2,3-NcH_2 molecule, including in-plane bending CH modes.

Acknowledgments

This work was performed with the partial financial support from the Belarusian Republican Foundation for Fundamental Research (Grant F03-072) and Programme de Bourses de Recherche Scientifique et Technique de l'OTAN (NATO/France-East European Countries).

References

[1] A.V. Turukhin, A.A. Gorokhovsky, C. Moser, I.V. Solomatin, D. Psaltis, J. Lumin. 86 (2000) 399.
[2] A.V. Turukhin, A.A. Gorokhovsky, Chem. Phys. Lett. 317 (2000) 109.
[3] T. Chanelière, S. Fraigne, J.-P. Galaup, M. Joffre, J.-L. Le Gouët, J.-P. Likforman, D. Ricard, Eur. Phys. J. AP 20 (2002) 205.
[4] S. Fraigne, J.-P. Galaup, J.-L. Le Gouët, B. Bousquest, L. Canioni, M. Joffre, J.-P. Likforman, J. Opt. Soc. Am. B 20 (2003) 1555.
[5] J.-P. Galaup, S. Fraigne, J.-L. Le Gouët, J.-P. Likforman, M. Joffre, J. Lumin. 107 (2004) 187.
[6] N. Kobayashi, in: K.M. Kadish, K.M. Smith, R. Guilard (Eds.), The Porphyrin Handbook, vol. 15, Academic Press, New York, 2003, p. 161.
[7] K. Ishii, N. Kobayashi, in: K.M. Kadish, K.M. Smith, R. Guilard (Eds.), The Porphyrin Handbook, vol. 16, Academic Press, New York, 2003, p. 1.
[8] S.A. Mikhalenko, E.A. Luk'yanets, Zh. Obshch. Khim. 39 (1969) 2554.
[9] M.L. Kaplan, A.J. Lovinger, W.D. Reents, P.H. Schmidt, Mol. Cryst. Liq. Cryst. 112 (1984) 345.
[10] I. Gobernado-Mitre, R. Aroca, J.A. De Saja, Chem. Mater. 7 (1995) 118.
[11] E.I. Kovshev, E.A. Luk'yanets, Zh. Obshch. Khim. 42 (1972) 696.
[12] I. Renge, H. Wolleb, H. Spahni, U.P. Wild, J. Phys. Chem. A 101 (1997) 6202.
[13] N. Kobayashi, Y. Higashi, T. Osa, Chem. Lett. (1994) 1813.
[14] M.J. Cook, A.J. Dunn, S.D. Howe, A.J. Thomson, K.J. Harrison, J. Chem. Soc. Perkin Trans. I (1988) 2453.
[15] K. Kitahara, T. Asano, K. Hamano, S. Tokita, H. Nishi, J. Heterocyclic Chem. 27 (1990) 2219.
[16] V.V. Sapunov, A.P. Tsvirko, K.N. Solovyov, Khim. Fizika 5 (1986) 948.
[17] V.V. Sapunov, Zh. Prikl. Spektrosk. 53 (1990) 819, [J. Appl. Spectrosc. 53 (1990) 1213].
[18] M.G. Gal'pern, T.D. Talismanova, L.G. Tomilova, E.A. Luk'yanets, Zh. Obshch. Khim. 55 (1985) 1099.
[19] E. Orti, M.C. Piqueras, R. Crespo, J.L. Bredas, Chem. Mater. 2 (1990) 110.
[20] A. Ghosh, P.G. Gassman, J. Almlöf, J. Am. Chem. Soc. 116 (1994) 1932.
[21] N. Kobayashi, H. Konami, in: C.C. Leznoff, A.B. Lever (Eds.), Phthalocyanines – Properties and Applications, vol. 4, VCH Publishers, New York, 1996 (Chapter 9).
[22] European Pat. Specification 0 054.992 D 06L3/04, 1981.
[23] E.I. Kovshev, V.A. Puchnova, E.A. Luk'yanets, Zh. Org. Khim. 7 (1971) 369.
[24] L.L. Hench, J.K. West, Chem. Rev. 90 (1990) 33.
[25] C.J. Brinker, G.W. Scherer, Sol–Gel Science: The Physics and Chemistry of Sol–Gel Processing, Academic Press, New York, 1990.
[26] S.M. Arabei, S.F. Shkirman, K.N. Solovyov, Spectrochim. Acta A 48 (1992) 155.
[27] S.A. Mikhalenko, S.V. Barkanova, O.L. Lebedev, E.A. Luk'yanets, Zh. Obshch. Khim. 41 (1971) 2735.
[28] V.A. Kuzmitsky, K.N. Solovyov, V.N. Knyukshto, I.K. Shushkevich, V.N. Kopranenkov, A.M. Vorotnikov, Teor. Eksp. Khim. 19 (1983) 655.
[29] V.A. Kuzmitsky, K.N. Solovyov, V.N. Kopranenkov, Zh. Prikl. Spektrosk. 49 (1988) 603, [J. Appl. Spectrosc. 49 (1988) 1037].
[30] V.N. Kopranenkov, A.M. Vorotnikov, S.N. Dashkevich, E.A. Luk'yanets, Zh. Obshch. Khim. 55 (1985) 900.
[31] I.K. Shushkevich, V.N. Knyukshto, S.N. Dashkevich, V.N. Kopranenkov, K.N. Solovyov, Teor. Eksp. Khim. 26 (1990) 92.
[32] G. Herzberg, Molecular Spectra and Molecular StructureElectronic Spectra and Electronic Structure of Polyatomic Molecules, vol. III, Van Nostrand, Princeton, New York, 1966, p. 66.
[33] V.N. Kotlo, K.N. Solovyov, S.F. Shkirman, I.E. Zalesskii, Vestsi Akad. Navuk BSSR. Ser. Fiz.-Mat. Navuk (3) (1974) 99; V.N. Kotlo, K.N. Solovyov, S.F. Shkirman, I.E. Zalesskii, Chem. Abstr. 81 (1974) 113223r.
[34] S.F. Shkirman, N.A. Sokolov, V.K. Konstantinova, K.N. Solovyov, Zh. Prikl. Spektrosk. 68 (2001) 315, [J. Appl. Spectrosc. 68 (2001) 410].
[35] W.-J. Huang, S. Salman, G. Jean-Charles, E. Van Riper, L.W. Johnson, Spectrochim. Acta A 52 (1996) 157.
[36] S.M. Arabei, K.N. Solovyov, E.A. Makarova, Zh. Prikl. Spektrosk. 71 (2004) 33.
[37] S. Völker, J.H. van der Waals, Mol. Phys. 32 (1976) 1703.
[38] I.V. Stanishevsky, K.N. Solovyov, Opt. Spektrosk. 96 (2004) 255, [Opt. Spectrosc. 96 (2004) 221].
[39] E.R. Lippincott, E.J. O'Reilly Jr., J. Chem. Phys. 23 (1955) 238.
[40] A.L. McClellan, G.C. Pimentel, J. Chem. Phys. 23 (1955) 245.
[41] H.F. Shurvell, L. Pinzuti, Can. J. Chem. 44 (1966) 125.
[42] R. Aroca, D.P. DiLella, R.O. Loutfy, J. Phys. Chem. Solids 43 (1982) 701.
[43] C. Jennings, R. Aroca, A.-M. Hor, R.O. Loutfy, J. Raman Spectrosc. 15 (1984) 34.
[44] R.I. Personov, Opt. Spektrosk. 15 (1963) 61.
[45] T.-H. Huang, K.-E. Rieckhoff, E.M. Voigt, J. Chem. Phys. 77 (1982) 3424.
[46] L.L. Gladkov, S.F. Shkirman, N.I. Sushko, V.K. Konstantinova, N.A. Sokolov, K.N. Solovyov, Spectrosc. Lett. 34 (2001) 709.
[47] L.L. Gladkov, V.K. Konstantinova, N.M. Ksenofontova, N.A. Sokolov, K.N. Solovyov, S.F. Shkirman, Zh. Prikl. Spektrosk. 69 (2002) 44, [J. Appl. Spectrosc. 69 (2002) 47].

[48] D.R. Tackley, G. Dent, W.E. Smith, Phys. Chem. Chem. Phys. 2 (2000) 3949.
[49] K.N. Solovyov, I.E. Zalesskii, V.N. Kotlo, S.F. Shkirman, Pis'ma Zh. Eksp. Teor. Fiz. 17 (1973) 463.
[50] A.A. Gorokhovskii, R.K. Kaarli, L.A. Rebane, Pis'ma Zh. Eksp. Teor. Fiz. 20 (1974) 474.
[51] I.E. Zalesskii, V.N. Kotlo, A.N. Sevchenko, K.N. Solovyov, S.F. Shkirman, Dokl. Akad. Nauk SSSR 207 (1972) 1314.
[52] R.I. Personov, in: V.M. Agranovich, R.M. Hochstrasser (Eds.), Spectroscopy and Excitation Dynamics of Condensed Molecular Systems, North-Holland, Amsterdam, 1983, p. 555.
[53] J. Bernard, M. Orrit, R.I. Personov, A.D. Samoilenko, Chem. Phys. Lett. 164 (1989) 377.
[54] H. Talon, M. Orrit, J. Bernard, Chem. Phys. 140 (1990) 177.
[55] I.V. Stanishevsky, K.N. Solovyov, Opt. Spektrosk. 97 (2004) 286, [Opt. Spectrosc. 97 (2004) 270].